The effect of coupled dynamic analysis of floater motions on the mooring and riser system response of a FPSO

Marcelo Caire and Rafael Vergara Schiller
MARINTEK do Brasil
marcelo.caire@marintek.com.br; rafael.schiller@marintek.com.br

Abstract

Floating unit, mooring lines and risers comprise an integrated dynamic system that responds to environmental loading due to wind, waves and currents in a complex way. The sea current forces acting on the moorings/risers and the resulting damping effects can be an important contribution for the floating unit response. For the integrity assessment of the riser system, one of the traditional methodologies employed is to consider wave frequency (WF) floater motion as dynamic excitation through the vessel Response Amplitude Operator (RAO), while low frequency (LF) floater motions are accounted for by an additional static offset. In deep waters, especially with a large number of slender structures supported by the vessel, it becomes increasingly important to consider the coupling effect between the floating unit, mooring lines and risers, since this can affect the motions of the platform and consequently the riser system response. In this paper, the coupled vs. de-coupled approaches for assessment of the riser system are evaluated by case studies of a deep water, spread-moored Floating, Production, Storage and Offloading unit (FPSO) operating in offshore Brazil. Analyses for floating unit response coupled with moorings/risers and the top connection response of the slender structures are presented and the two approaches are compared.

Keywords

Coupled analysis, FPSO, flexible risers, mooring lines, damping.

Nomenclature

$\mathbf{M}$	Frequency-dependent mass matrix
$\mathbf{A}$	Frequency-dependent added mass matrix
$\mathbf{D}_1$	Linear damping matrix
$\mathbf{K}$	Hydrostatic stiffness matrix
$\mathbf{q}$	Exciting force vector
$\mathbf{q}_{WA,1}$	1st order wave excitation force vector
$\mathbf{q}_{CU}$	Current drag force vector
$\mathbf{h}$	Retardation function vector
$\mathbf{R}^D$	Finite element model damping force vector
$\mathbf{R}^E$	Finite element model external force vector
t	Time
$\mathbf{m}$	Rigid-body mass matrix
$\mathbf{C}$	Frequency-dependent potential damping matrix
$\mathbf{D}_2$	Quadratic damping matrix
$\mathbf{x}$	Vessel position vector
$\mathbf{q}_{WI}$	Wind drag force vector
$\mathbf{q}_{WA,2}$	2nd order wave excitation force vector
$\mathbf{q}_{EXIT}$	Specified forces and forces from station keeping and coupling elements vector
$\mathbf{R}^I$	Finite element model inertia force vector
$\mathbf{R}^S$	Finite element model structural reaction force vector
$\mathbf{r},\dot{\mathbf{r}},\ddot{\mathbf{r}}$	Structural displacement, velocity and acceleration vectors

Submitted to MS&OT on November 21 2012. Accepted on December 07 2012. Editor: ***Marcelo A. S. Neves****.*

1 Introduction

As the oil and gas Industry moves toward deeper waters, traditional numerical methods for global dynamic analysis of the floating unit, mooring lines and riser system may no longer be adequate. Traditional methods tend to assess the dynamics of the floating unit and of the moorings/risers separately, therefore not taking into account coupling effects between both systems. Although such approach may be acceptable for shallow waters, coupling effects become increasingly more important in deep waters as observed by Gonzales et al. (2005) and Torres et al. (2008). The importance of coupling effects between the floating unit and the moorings-risers system in deep waters has been shown in previous studies for different structures, such as semi-submersibles, TLPs, SPARs and FPSOs (e.g. Ormberg and Larsen (1998); Ormberg et al. (1997, 1998, 2003, 2005); Chaudhury and Ho (2000); Colby et al. (2000); Astrup et al. (2001); Rodrigues et al. (2008),among others).

It is observed that, in deep waters, coupling effects associated with moorings and risers improve the predictions of floater motions. LF motions are usually reduced due to the correct prediction of inertial and damping effects from the slender structure system, and the mean offset is accurately enhanced due to the current loads acting on the moorings and risers. Moreover, the interactions between WF and LF responses are automatically taken into account. One of the feedbacks on the moorings and risers is a better prediction of top connection boundary displacements. Therefore, it is expected that the corrections associated with a coupled analysis will reflect in a better prediction of riser system structural integrity assessment.

The response analysis of a flexible riser system of an FPSO may be influenced by several aspects, such as: a) coupled analysis of the global dynamics of riser systems; b) bi-directional and bi-modal seas with wave energy directional spreading; c) bending moment x curvature hysteresis of flexible risers and d) time-dependent behavior of bend stiffeners. From the environmental point of view, (b) is extremely relevant for sea states in offshore SE Brazil, in particular for the Campos and Santos Basins where S-SW swell-seas may be observed in combination with N-NE wind-seas as discussed by Vogel et al. (2010). Material non-linearities may be very important for flexible risers and umbilical cables where a (c) hysteretic bending moment x curvature response is present due to the interlayer contact. As shown by Smith et al. (2007), accounting for hysteresis in the global motion analysis can be essential in demonstrating a safe riser fatigue life. From the local point of view, (d) is important because current practice in bend stiffeners analysis does not take into account the rate dependent response and damping of the polyurethane, which may significantly affect the riser curvature distribution at top connection as shown by Caire (2011). Although it is not expected to present significant influence in the global response, the local cross section analysis of the pipe can be highly affected by the bend stiffener model.

In the present work we focus on (a) and our objective is to investigate the effect of a coupled analysis on the global dynamics of a floater-mooring-riser system. Our study case is a typical FPSO with 20 spread-mooring lines and 15 flexible risers, operating in a water depth of 1250m in offshore SE Brazil. A selection of environmental states representative of the Campos Basin is used, and an investigation of the top tension and displacement results from de-coupled and coupled analyses is performed.

2 Global dynamic analysis methodologies for riser integrity assessment

2.1 De-coupled methodologies

The dynamic analysis of a complete offshore floating system, including the floater motions and the dynamic response of risers and mooring lines (hereafter also referred as slender structures), has been traditionally carried out in two steps. In the so-called de-coupled methodology, the motions of the floater are firstly simulated with a simplification of the forces from the mooring lines and risers. The static restoring forces from slender structures may be properly accounted for by assuming non-linear springs, but damping and inertial forces can only be included in a simplified way. Secondly, the simulated floater motions are imposed as top-end boundary conditions in the calculation of dynamic loads of the mooring lines and risers. In this second step, the responses of the slender structures cannot modify the floater motions. The de-coupled analysis is schematically presented in Figure 1.

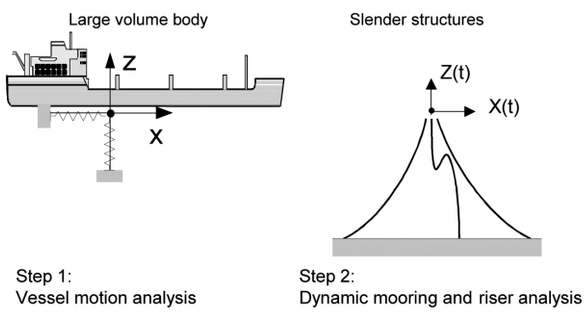

Fig. 1 De-coupled analysis approach (adapted from Ormberg et al. (2005)).

With respect to an exclusive mooring-riser analysis without a time-domain simulation of the vessel motions, a de-coupled approach is also the traditional methodology used by the Industry. In such de-coupled mooring-riser analysis, the calculation of the dynamic loads takes into account (Rodrigues et al. (2008)): a) Vessel WF motions, calculated from response amplitude operators (RAOs) obtained from diffraction analysis and b) Representative offset (mean plus LF). The offset can be obtained from a frequency-domain static / dynamic analysis of

the floater-slender structure system. It is important to point out that other analysis methodologies may also be employed, which includes the use of both WF and LF response amplitude operators.

2.2 Coupled analysis methodology

Coupling effects between the floater and the slender structures may be defined as "the influence on floater mean position and dynamic response due to slender structure restoring, damping and inertia forces" as described by Astrup et al. (2001). The proper coupling between the floater and slender structures is obtained in the so-called coupled analysis. In this approach, the floater simulation is performed simultaneously with the simulation of the slender structures. The dynamic simulation of moorings and risers will provide accurate forces to the floater simulation, and the latter will provide the correct motions to the former. The coupled analysis is schematically presented in Figure 2. A coupled analysis will take into account the following coupled effects from the moorings and risers:

i. Static restoring forces related to current loading, sea floor friction and displacement;

ii. Damping forces due to the dynamics of the slender structures (Morison forces and energy loss due to flexible riser interlayer friction) and related to hull-riser contact;

iii. Inertia forces also related to the dynamics.

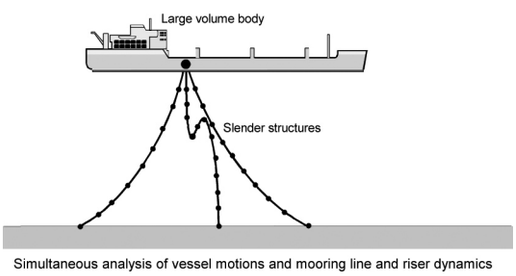

Fig. 2 Coupled analysis approach (adapted from Ormberg et al. (2005)).

Below follows a brief description of the model components that simulate the time-domain dynamics of the floater, of the slender structures, and of the coupling between them. More details can be found in Ormberg et al. (1997, 1998, 2005) and Ormberg and Larsen (1998). Overall procedures for coupled analyses can be found in DNV-RP-F205 (2004).

2.2 (a) Non-linear time domain floater model

The floater's dynamics is modeled in a non-linear, time-domain fashion by use of SIMO (2012), a tool for simulation of motions and station-keeping behavior of floating vessels and suspended loads. SIMO allows flexible modeling of multi-body systems, with non-linear time-domain simulation of floating systems under environmental loads due to wind, waves and current, besides passive and active positioning forces (anchor lines, wires, hawsers, thrusters, fenders, etc). The 6 degrees-of-freedom (DOF) equation of motions for a rigid floating body is (Bailey et al., 1997):

$$(\mathbf{m}+\mathbf{A}_{\infty})\ddot{\mathbf{x}}+\mathbf{D}_1\dot{\mathbf{x}}+\mathbf{D}_2\dot{\mathbf{x}}\left|\dot{\mathbf{x}}\right|+\mathbf{K}\mathbf{x}+\int_{-\infty}^{t}\mathbf{h}(t-\tau)\dot{\mathbf{x}}(\tau)\mathbf{d}\tau=\mathbf{q}(t,\dot{\mathbf{x}},\ddot{\mathbf{x}}) \quad (1)$$

where $\mathbf{A}_{\infty}=\mathbf{A}(\omega\to\infty)$ is the infinity-frequency added mass matrix and the convolution integral comprises radiation forces due to frequency-dependent added mass and damping (Cummins (1962)). Potential theory is applied for evaluation of the interaction between waves and the floater. Radiation and diffraction loads are considered by means of coefficients and transfer functions calculated by a Boundary Element Method (BEM-based) solver, e.g. WAMIT (2012). The retardation function **h** is given by:

$$\mathbf{h}(\tau)=\frac{1}{\pi}\int_0^{\infty}[\mathbf{C}(\omega)\cos(\omega\tau)-\omega\mathbf{A}(\omega)\sin(\omega\tau)]d\omega \quad (2)$$

For $\tau > 0$, the wave forces are calculated for a range of headings to allow for large yaw motion. Direction-dependent coefficients are used to calculate quadratic wind and current forces which are a function of wind and current direction with respect to the floater. The exciting forces on the right-hand side of Eq. (1) is then defined according to:

$$\mathbf{q}(t,\dot{\mathbf{x}},\ddot{\mathbf{x}})=\mathbf{q}_{\mathbf{WI}}+\mathbf{q}_{\mathbf{WA,1}}+\mathbf{q}_{\mathbf{WA,2}}+\mathbf{q}_{\mathbf{CU}}+\mathbf{q}_{\mathbf{EXT}} \quad (3)$$

Further details on the numerical methods adopted for calculating the terms on Eq. (3) can be found in SIMO (2012).

2.2 (b) Slender structure non-linear finite element model

The non-linear time-domain dynamics of mooring lines and risers are modeled in RIFLEX (2012), a tool for the analysis of multiple types of slender structures, such as flexible marine riser systems, mooring lines, umbilicals, steel pipelines and conventional risers. Based on a non-linear finite element (FE) formulation using beam and bar element types, RIFLEX allows for large deflections and rotations, large upper-end motion excitation and non-linear cross-section properties. Mooring lines usually employ 3D, 6 DOF bar-cable elements. For risers systems where bending stiffness is important, 3D, 12 DOF beam elements are employed. The load model for the slender structures considers the weight, buoyancy, internal flow and hydrodynamic forces, the latter being modeled by means of the generalized Morison's equation and specifying added mass and drag coefficients for each element. Spring and friction models represent the seabed contact. The governing dynamic equilibrium equation of the spatially discrete, FE system may be expressed by:

$$\mathbf{R}^{\mathbf{I}}(\mathbf{r},\ddot{\mathbf{r}},t)+\mathbf{R}^{\mathbf{D}}(\mathbf{r},\dot{\mathbf{r}},t)+\mathbf{R}^{\mathbf{S}}(\mathbf{r},t)=\mathbf{R}^{\mathbf{E}}(\mathbf{r},\dot{\mathbf{r}},t) \quad (4)$$

The inertia force vector is given by,

$$\mathbf{R}^{\mathbf{I}}(\mathbf{r},\ddot{\mathbf{r}},t)=\mathbf{M}(\mathbf{r})\ddot{\mathbf{r}} \quad (5)$$

where the mass matrix accounts for structural mass, internal fluid flow and hydrodynamic mass. The damping force vector can be expressed as follows,

$$\mathbf{R}^{\mathbf{D}}(\mathbf{r},\dot{\mathbf{r}},t) = \mathbf{C}(\mathbf{r})\dot{\mathbf{r}} \tag{6}$$

where the damping matrix includes contributions from internal structural damping and also allows discrete dashpot dampers to be modeled. The internal structural damping must be included in the dynamic analysis to account for the energy dissipation related to axial, torsional and bending deformations. A very low viscous damping is observed for axial and torsional deformations, being usually disregarded. As previously mentioned, the flexible riser interlayer friction leads to an amplitude dependent hysteretic type of damping. This energy loss may present some impact in the global dynamic analysis, especially for floating units operating in deep water with a large number of risers supported.

The external load vector $\mathbf{R}^{\mathbf{E}}$ accounts for weight, buoyancy, forced displacements, environmental forces and specified forces. The numerical method to solve (4) is based on an incremental solution procedure using the dynamic time integration scheme according to the Newmark β-family. A Newton-Raphson interation method is used to achieve dynamic equilibrium. More details on the numerical methods can be found in Ormberg et al. (2005) and in RIFLEX (2012).

2.2 (c) Coupled floater / slender structure model

In the coupled analysis, SIMO and RIFLEX are executed simultaneously. The floater is modeled as a one-node rigid element with 6 DOF in the slender structure FE model. The forces on the vessel are computed separately for each time step and included in the external load vector $\mathbf{R}^{\mathbf{E}}$. Vessel inertia forces representing the vessel mass and the frequency-independent part of the added mass are included in the mass matrix of Eq. (4).

3 Case study definition

3.1 FPSO-riser-mooring system

In the present work, we employ a standard FPSO model with a spread-mooring system that consists of 20 mooring lines. For FPSOs that are anchored with this system, the risers are connected to a balcony on one side of the hull, leaving the other side for cargo handling and the approach of supply vessels. For the current FPSO, 15 risers are connected to port side, leaving the starboard side free. One group of risers has a touch-down point to the starboard side of the floater, while another group has a touch-down point to the port side of the floater. With respect to the riser system, a 2.5'' ID flexible pipe has been selected for the present case study. The main properties can be seen in Table 1 while more detailed information about this cross-section can be found in Witz (1996).

Table 1 Flexible riser properties.

Property	Unit	Value
Internal diameter	mm	63.20
External diameter	mm	111.5
Axial stiffness	MN	128.00
Bending stiffness	Nm^2	1190.00
Torsional stiffness	kNm^2/rad	203.00
Mass in air	Kg/m	30.43

The mooring system consists of 20 spread-moored lines, where 5 are located at the bow-starboard side, 5 at the bow-port side, 5 at the stern-starboard side and 5 at the stern-port side. Each mooring line is comprised by three segments: two chain segments and one polyester line. Relevant mooring properties can be found in Wibner et al. (2003).

The slender structure finite element model of the mooring lines and risers is the most computationally intensive process and, consequently, governs the efficiency and stability of the coupled analysis. A proper selection of the mesh is essential to capture the coupling effects while having an analysis that is numerically efficient. In the present case study, all mooring lines and riser were modeled using bar elements; hence, no bending stiffness was considered for the risers. 161 elements were used to represent each mooring line, while 289 elements were employed to represent each flexible riser, comprising a total of 7555 elements in the FE discretization. Figure 3 shows a schematic representation of the slender structure system in its static configuration.

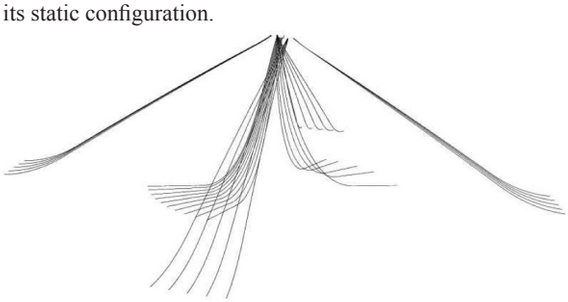

Fig. 3 Moorings and risers layout.

3.2 Environmental loading and cases definition

The environmental conditions adopted in this study are representative of typical sea states from Campos Basin, in SE offshore Brazil. A water depth of 1250m is considered. We select wave and current scenarios for a return period of 10 years. The convention adopted is as follows: i) for waves, the direction indicates where they come from and ii) for current, the direction indicates where it goes to (relative to true north, clockwise rotation). The vessel is considered to be moored with a southwesterly heading of 225 degrees clockwise (relative to true north). The wave and current directions that were selected for this study are shown in Figure 4.

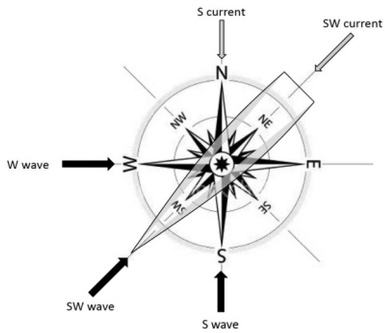

Fig. 4 Schematic representation of the vessel heading and directions of waves and currents.

Irregular waves are represented by a JONSWAP spectrum, which is defined by the significant wave height Hs, peak period Tp and peak enhancement parameter γ. Table 2 shows the three wave directions employed in this study, with their respective wave parameters. S and SW waves are selected because they represent the largest and longest waves in the Campos Basin. Those are representative of swell waves associated with extra-tropical storm activity (Vogel et al. (2010)). W waves are representative of wind waves and are selected as an example of smaller and shorter waves.

Table 2 Wave data.

Direction	Hs (m)	Tp (s)	γ
S	6.1	14.00	1.57
SW	6.9	14.62	1.61
W	4.0	8.14	2.10

Two scenarios of surface currents are selected, S and SW (Table 3). S and SW surface currents are associated with the prevailing direction of the Brazil Current, the dominant current system in the Campos Basin as discussed by Silveira (2007). For simplicity, the current direction is constant throughout the water column, with a maximum speed at the surface and a linear decay to zero at the bottom.

Table 3 Surface current data.

Direction	Speed (m/s)
S	1.58
SW	1.39

As shown in Table 4, six loading cases were defined using the above wave and current data. Loads due to wind are not included in the present analysis.

Table 4 Loading cases.

Case	Wave	Current
01	S	SW
02	SW	SW
03	W	SW
04	S	S
05	SW	S
06	W	S

3.3 FPSO-riser-mooring system

Coupled and de-coupled analyses were performed for all load cases. Instead of using the traditional frequency domain analysis to estimate the representative offset for a given environmental condition, the following procedure was employed: i) perform a coupled simulation for a (short) 1h period; ii) compute the average offset of the floater and iii) perform a 1h de-coupled simulation with the average offset previously estimated. Based on the 1h coupled simulations, the case with the worst load on the riser system is selected for a detailed comparison between the coupled and de-coupled approaches. This comparison is made by performing coupled and de-coupled simulations that are representative of a 6h period.

4 Results

4.1 Estimation of the average offset for the de-coupled analysis

Figures 5 to 10 show the floater trajectory for all loading cases from the 1h coupled simulations. The initial position is (0,0), and the trajectories are given in global coordinates. For all cases, it is observed an initial displacement towards a preferred direction within the first 6 minutes of simulation. This initial displacement corroborates with the direction of the current, suggesting that the current dominates the trajectory of the floater until an equilibrium position is achieved. One exception is case 02 (Figure 6), where waves and currents are in opposite directions but aligned with the major axis of the floater.

After this equilibrium point is achieved, the horizontal position of the floater is largely dominated by LF oscillations in surge and sway. Here, LF motions are represented by wave drift forces. Based on the spectrum of surge and sway motions (Figures 11 and 12) and on the trajectories, one can observe that cases 01 and 04 are largely modulated by a combination of surge and sway drifts, cases 02 and 05 are largely modulated by surge, and cases 03 and 06 are largely modulated by sway.

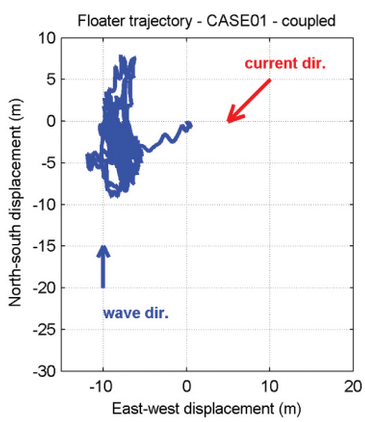

Fig. 5 Case 01 floater trajectory from the 1h coupled simulations.

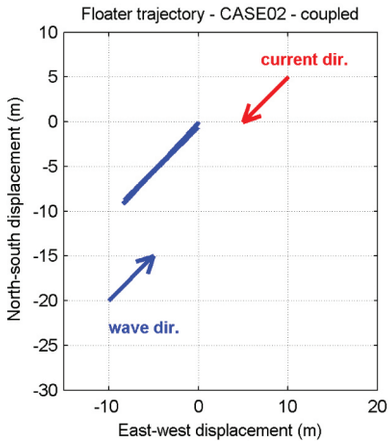

Fig. 6 Same as Fig. 5, but for case 02.

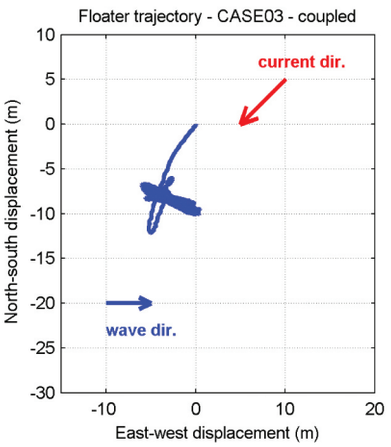

Fig. 7 Same as Fig. 5, but for case 03.

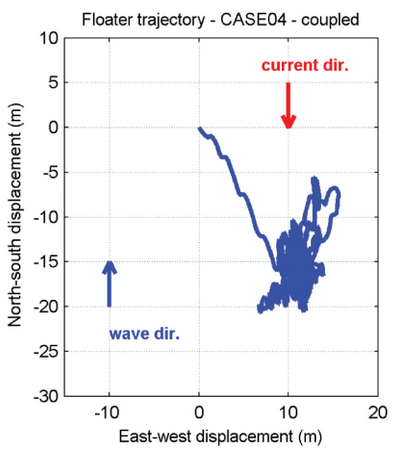

Fig. 8 Same as Fig. 5, but for case 04.

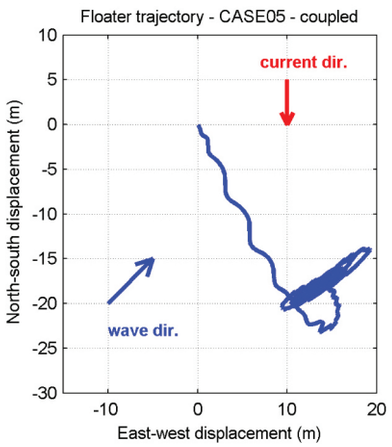

Fig. 9 Same as Fig. 5, but for case 05.

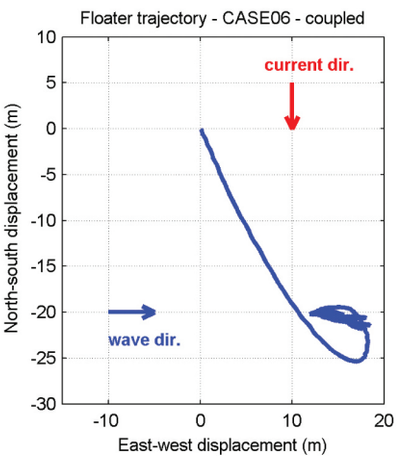

Fig. 10 Same as Fig. 5, but for case 06.

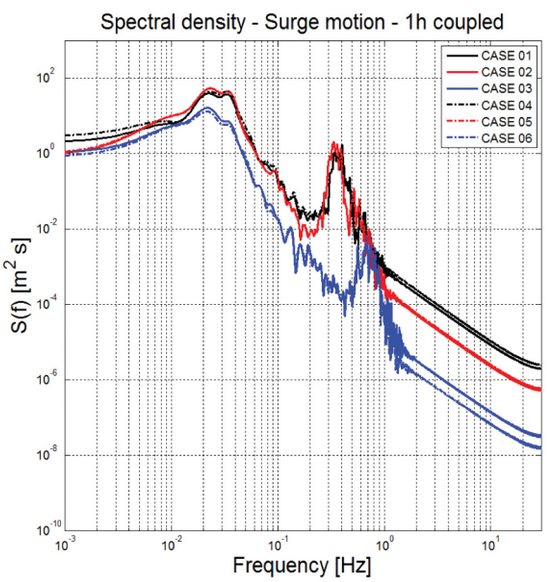

Fig. 11 Surge motion spectral density.

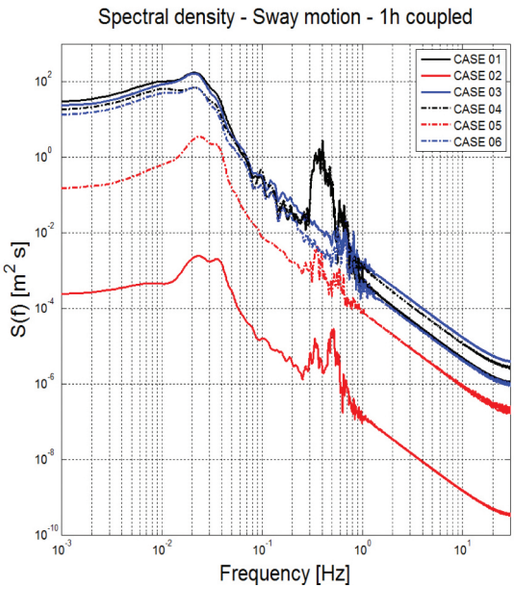

Fig. 12 Sway motion spectral density.

The average offset (x,y) for each coupled simulation is presented on Table 5. That offset is computed in vessel coordinates, and it represents the average surge and sway displacements after the 1h simulations. The final distance from the initial point is also shown. Overall, the largest offsets are observed for S currents, in special for case 06, where both waves and currents contribute to a large displacement to SW.

Figure 13 shows the time-average top tension of the mooring lines for all 1h coupled simulations. One can observe that, in agreement with the floater trajectories, the largest mean top tensions occur for the loading cases with southward (S) currents (largest offsets). The largest mean top tensions are observed for the group of mooring lines on stern-starboard side of the floater (lines #6 to #10).

Table 5 Mean representative offset in vessel coordinate system.

Case	x (m)	y (m)	Distance (m)
01	7.4	-3.7	8.27
02	7.5	0.35	7.50
03	8.0	3.5	8.73
04	3.2	18.6	18.87
05	3.4	22.0	22.26
06	3.9	24.8	25.10

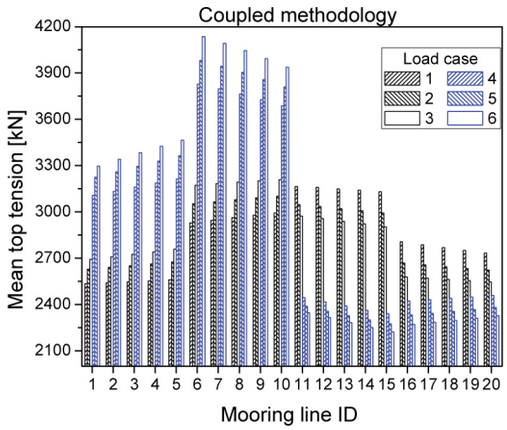

Fig.13 Mean top tension of the risers for all loading cases from the 1h coupled simulations.

Figure 14 shows the time-average top tension of the risers for all 1h coupled simulations. Patterns similar to the ones from Fig. 13 are observed. Again, the largest values for the mean top tension are observed for southward currents (cases 04 to 06) and for the group of risers with the touch-down point to the starboard of the floater (risers #11 to #15).

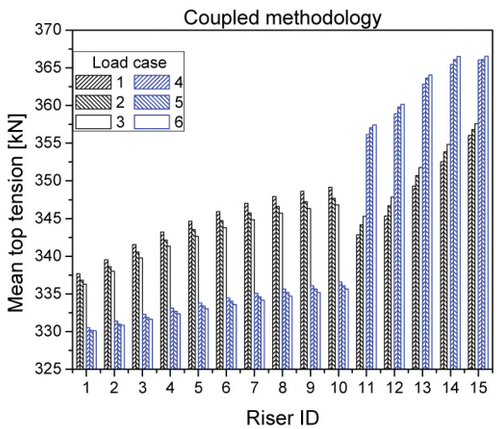

Fig.14 Mean top tension of the risers for all loading cases from the 1h coupled simulations.

4.2 Floating unit response coupled with moorings/risers

Based on the results from the 1h coupled simulations, we selected case 06 as the case with the worst environmental load. The mean offset of case 06 is used in a longer de-coupled simulation for a detailed comparison with the coupled approach.

Figure 15 shows the surge, sway and heave floating unit response coupled with the riser and mooring system for a 1h period selection from the 6h simulation. As expected, the

surge and sway responses are dominated by the low frequency response, while the heave response is dominated by the wave frequency excitation. The heave time series present a negative mean value due to riser and mooring system downward forces.

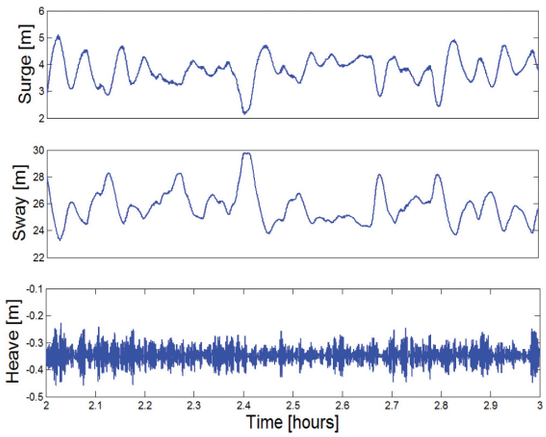

Fig.15 Surge, sway and heave vessel response for case 06.

In Fig. 16 the roll, pitch and yaw responses are presented. In the static equilibrium configuration with risers/moorings, the floating unit presents an asymmetric roll angle towards the side where the risers are hanging off (port side). The procedure adopted in this work is to add ballast on the opposite side (starboard) in such a manner that the roll response will be zero at the start of the dynamic analysis. The dynamic roll response presents a positive mean value indicating that, for the specific loading case #6, the current loading (Morison forces) acting on the submerse riser system leads to a resultant downward force in the hang off connection.

In the fully coupled analysis, the vessel heading will vary according to each short term environmental condition. In Fig. 16 it can be observed that the yaw response has a mean negative value, showing that the case 06 loading leads to a head change to starboard side.

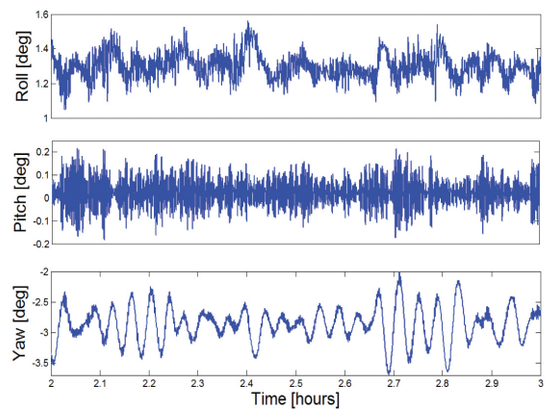

Fig.16 Roll, pitch and yaw vessel response for case 06.

In Fig. 17 a numerical free decay roll test is presented for the FPSO with and without risers. The viscous roll damping (without risers) was adjusted using the results presented by Veer and Fathi (2011). They have shown that the riser balcony on one side of the vessel contributes to the roll damping through similar physics as the bilge keel does. For that purpose, a constant moment is applied in the static analysis and released for the dynamic simulation. It can be observed that the moorings/risers lead to increased damping in the vessel response, as well as a natural period change. This increased damping, which is intrinsically considered in a fully coupled time domain simulation, may impact the riser system response and consequently its fatigue life estimation.

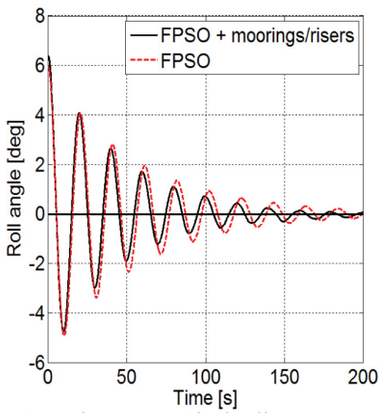

Fig. 17 Free decay numerical roll response.

4.3 Mooring system response

The detailed comparison between the de-coupled and coupled approaches is done for 6h-long simulations. The environmental load is from case 06. Comparisons are made with respect to the response of mooring lines and risers. Figure 18 shows the time-average top tension of the mooring lines from both coupled and de-coupled approaches. Firstly, one observes that the results from the coupled 6h simulation are not significantly different from the results of the coupled 1h simulation (Figure 13). For the group of lines with the largest top tensions (#6 to #10), the coupled analysis presents slightly larger values than the de-coupled analysis. For lines #6 to #10, the de-coupled simulation under-estimates the tension by approximately 3-5%. Conversely, the de-coupled analysis presented larger values for other lines (#1 to #5, for example).

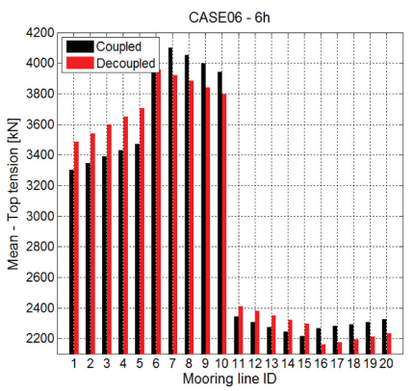

Fig.18 Mean top tension of the mooring lines from the 6h coupled and de-coupled simulations.

The standard deviation of the top tension of the mooring lines is higher for all mooring lines in the coupled approach (Figure

19). That is due to the correct inclusion of LF floater motions. Although the de-coupled simulation employs the mean offset to account for the lack of floater LF motions, the standard deviation is under-predicted. For the lines with the largest mean top tension (#6 to #10), the de-coupled simulations under-predict the standard deviation by about 75 - 80%.

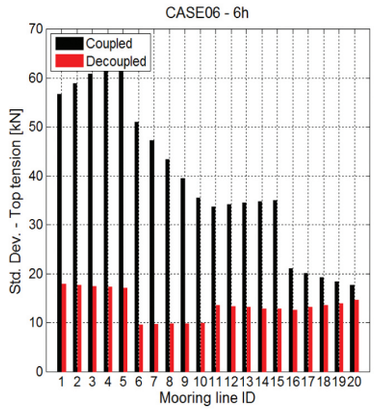

Fig.19 Top tension standard deviation of the mooring lines from the 6h coupled and de-coupled simulations.

We select two mooring lines to illustrate the temporal variations of top tension from the coupled and de-coupled approaches. The time series of top tension for the line with the largest mean tension (line #6) is shown in Figure 20. The distinctions between the time series are clear, as the de-coupled simulation shows an exclusive WF variability and the coupled simulation shows a dominant LF variability. Due to the highly dependent response on the LF motions, a higher deviation can be observed in the time series for the coupled approach. The same patterns are observed for line #1 (Figure 21), where the mean top tension from the de-coupled simulation is slightly larger.

The mean value deviations are mainly explained by the fact that in the coupled analysis, the vessel presents a heading variation according to each short term loading condition. As for case 06 the vessel presents a dominant head change to starboard side, and the moorings located in the stern-starboard side (mooring #6) will present a higher top tension when compared to the others located at the stern-port side.

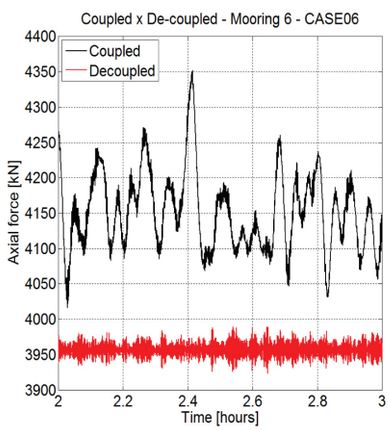

Fig.20 Time series of top tension of mooring line #6 for the 6h coupled and de-coupled simulations.

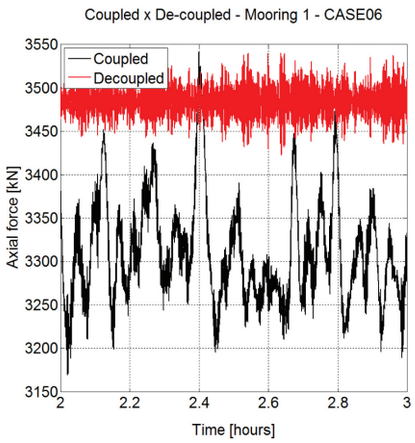

Fig.21 Time series of top tension of mooring line #1 for the 6h coupled and de-coupled simulations.

The top tension spectral density of the time series presented in Figure 20 (mooring #6) is shown in Figure 22 for both coupled and de-coupled simulations. For the coupled simulation the spectrum presents a peak value at ~300s and a lower one in the WF range close to 12s that coincides with the higher peak of the de-coupled simulation. The results confirm that the low frequency excitation dominates the mooring line response with small influence from the wave frequency range. For the de-coupled approach, where the surge and sway slow drift motions is not included, the energy is concentrated in the WF part of the spectrum.

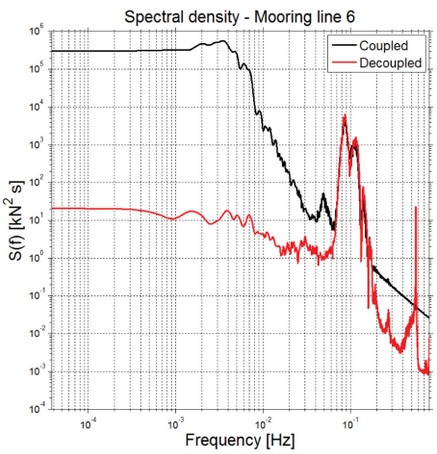

Fig.22 Top tension spectral density for mooring line #6 from the 6h coupled and de-coupled simulation.

4.4 Riser system response

The response of the riser system in the 6h coupled and de-coupled simulations are shown in this section. The time-average top tension of the risers in the 6h coupled simulation (Figure 23) is very similar to the results from the 1h coupled simulation (Figure 14). More importantly, the estimates of

mean top tension from the coupled simulation are very similar to the estimates from the de-coupled simulation. This result suggests that the riser response is less dependent on the LF excitation than the mooring lines.

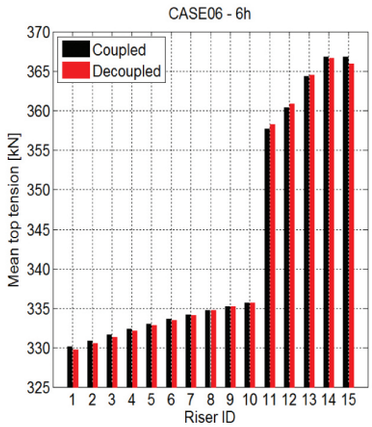

Fig. 23 Mean top tension of the riser system from the 6h coupled and de-coupled simulations.

The standard deviation of the top tension time series of the riser system (Figure 24) shows that, with the exception of riser #10, the standard deviation is higher for all de-coupled analyses. For the risers with the largest mean top tension (#11 to #15), the de-coupled simulations predict higher standard deviations by about 75-80%.

The results for standard deviation corroborate with the suggestion that the riser system was less subject to LF variability. Therefore, the riser system should be dominated by WF variability in both de-coupled and coupled simulations. Given that the floater WF motion may be reduced in the coupled simulation due to the coupling to the riser and mooring system, it is reasonable to have a larger standard deviation of riser top tension in the de-coupled simulation. From the point of view of riser fatigue analysis, this result indicates that the de-coupled approach could lead to a larger damage than what would be estimated by the coupled approach. Further investigation is required.

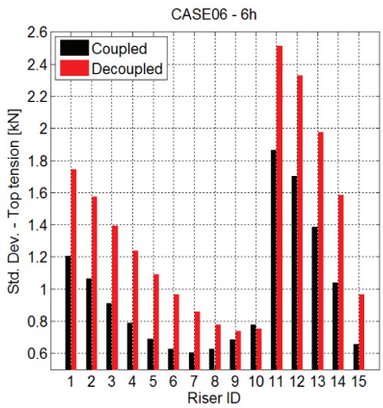

Fig. 24 Top tension std. deviation of the riser system from the 6h coupled and de-coupled simulations.

In spite of the differences in the estimates of standard deviation, it is important to point out the satisfactory agreement of the de-coupled approach to the coupled approach. Such reasonable agreement is achieved by using a representative offset whose computation takes into account the effects of LF floater motions from the non-linear, time domain coupled analysis. The traditional methodology is to employ linearized, frequency-domain analysis where the riser system is not included, using tools such as MIMOSA (2012).

The time series of top tension for the riser with the largest mean tension (riser #15) is shown in Figure 25 for both coupled and de-coupled analyses. In this case, differences are less noticeable due to the dominance of WF variability in both approaches. A comparison of the spectral density for both time series (Figure 26) shows the attenuation of the spectrum in the coupled analysis, which is related to the coupling effects between the floater, mooring lines and risers. It leads to a more spread energy distribution with a peak in the low frequency region.

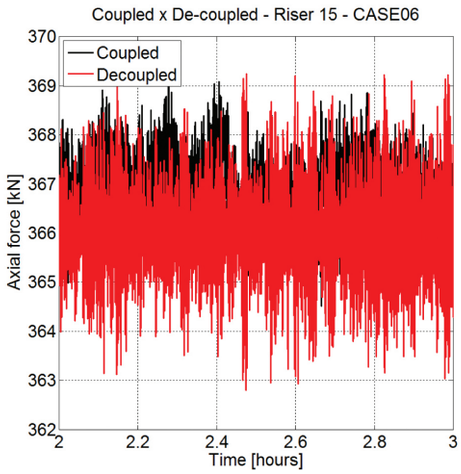

Fig.25 Time series of top tension of riser #15 for the 6h coupled and de-coupled simulations.

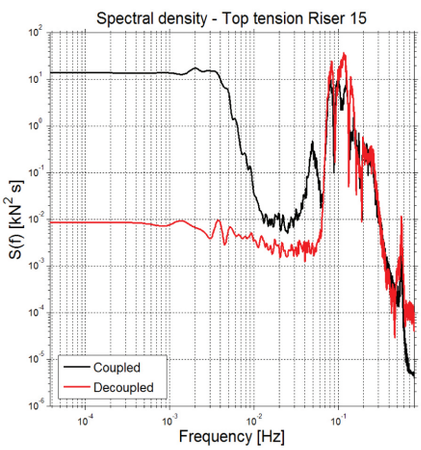

Fig. 26 Top tension spectral density for riser #15 from the 6h coupled and de-coupled simulations.

5 Summary and conclusions

A method for coupled motion analysis of floating moored structures and for the mooring line/riser system is outlined and applied to a case study of a typical spread-moored FPSO operating in offshore Brazil. The coupled approach is compared to one of the current practices of the Industry by applying the de-coupled approach (exclusive mooring-riser analysis using RAOs). From the case study presented herein, the main observations and conclusions are as follows:

i. The mooring and riser system increase the floating unit damping.

ii. The effect of current acting on moorings/risers may lead to an asymmetric response of the floating unit.

iii. The vessel heading is correctly taken into account in the coupled approach. There is no need for a separate heading distribution calculation as would be the case for the moorings/risers analysis in the de-coupled approach.

iv. For the mooring lines, higher standard deviations are observed for the coupled approach while the opposite occurs for the riser system, where the de-coupled simulations lead to higher values of standard deviation.

v. The mooring line top tension response is highly dependent on low frequency components, as expected.

In general terms, the coupled approach lowers the level of analysis uncertainties with a more physically correct modeling when compared to de-coupled methodologies. It is important to point out that this work concentrated on the dynamics of moorings and risers for a spread-moored FPSO system. Different results may be expected for other types of floating systems, such as semi-submersibles, which might have dynamic interactions between the floater and the lines that are different. The same can be said for different riser configurations (lines with submerged buoys, for example).

6 Acknowledgement

The authors would like to acknowledge the support of CNPq through the program "RHAE Researcher in the Company" (561416/2010-9), where a fellowship was provided for one of the authors (Rafael V. Schiller). The authors would also like to express their gratitude to João Paulo Cortina for his contribution to this work.

References

Astrup, O. C.; Nestegård, A.; Ronæss, M.; Sødahl, N. (2001) - "Coupled analysis strategies for deepwater spar platforms". In: 11th Annual International Offshore and Polar Engineering Conference (ISOPE), Stavanger, Norway.

Bailey, P. A.; Price, W. G.; Temarel, p. (1997) - "A unified mathematical model describing the maneuvering of a ship travelling in a seaway". Transactions of the Royal Institution of Naval Architects, 140, pp. 131-139.

Caire, M. (2011) – "Viscoelastic behavior modeling of bend stiffeners", DSc. Thesis (in portuguese), UFRJ, Rio de Janeiro, Brazil.

Chaudhury, G.; Ho, C-Yo. (2000) - "Coupled dynamic analysis of platforms, risers and moorings". In: Offshore Technology Conference (OTC) , Houston, USA, OTC-12084.

Colby, C.; Sødahl, N.; Katla, E.; Okkenhaug, S. (2000) - "Coupling effects for a Deepwater Spar", In: Offshore Technology Conference (OTC), 2000, Houston, USA, OTC-12083.

Cummins, W. E. (1962) - "The impulse response function and ship motions". David Taylor Model Basin, USA.

DNV-RP-F205 (2004) - "Recommended Practice - Global Performance Analysis of Deepwater Floating Structures".

Gonzalez, E.. Mourelle, M.M.; Mauricio, J.; Lima T.G.; Moreira C. C. (2005) - "Steel catenary riser design and analysis for Petrobras roncador field development". In: Offshore Technology Conference (OTC), Houston, USA, OTC-17670.

Mimosa (2012) - Program Documentation. SINTEF, Trondheim, Norway.

Ormberg, H.; Baarholm, R.; Stansberg, C. T. (2003) - "Time-domain coupled analysis of deepwater TLP, and Verification against Model Tests". In: 13th Annual International Offshore and Polar Engineering Conference (ISOPE), Honolulu, USA.

Ormberg, H.; Fylling, I. J.; Larsen, K., Sødahl, N. (1997) - "Coupled analysis of floater motion and mooring dynamics for a turret moored ship". In: 16th International Conference on Offshore Mechanics and Artic Engineering (OMAE), Yokohama, Japan.

Ormberg, H.; Larsen, K. (1998) - "Coupled analysis of floater motion and mooring dynamics for a turret-moored ship". Applied Ocean Research, Volume 20, pages 55-67.

Ormberg, H.; Lie, H.; Stansberg, C. T. (2005) - "Coupled analysis of offshore floating systems". Advances in Fluid Mechanics, Volume 42, pages 389-429.

Ormberg, H.; Sødahl, N.; Steinkjer, O. (1998) - "Efficient analysis of mooring systems using de-coupled and coupled analysis". In: 17th International Conference on Offshore Mechanics and Arctic Engineering (OMAE), Lisbon, Portugal, OMAE98-0351.

Van 'T Veer, R.; Fathi, F. (2011) - "On the roll damping of an FPSO with riser balcony and bilge keels". Transactions RINA, Vol 153, Part A2, International Journal Maritime Engineering.

RIFLEX (2012), Program Documentation. SINTEF, Trondheim, Norway.

Rodrigues, M.V.; Bahiense, R.A.; Steinkjer, O.; Raposo, C.V. (2008) - "Steel catenary riser design based on coupled analysis methodology". In: 27th International Conference on Offshore Mechanics and Arctic Engineering (OMAE), 2008, Estoril, Portugal, OMAE2008-57365.

Silveira, I. C. A. (2007) - "The Brazil current system in Campos basin", Thesis (in portuguese). USP, São Paulo, Brasil.

SIMO (2012) - Program Documentation. SINTEF, Trondheim, Norway.

Smith, R.; O'brien, P.; O'sullivan, T.; Weibe, C. (2007) - "Fatigue analysis of unbounded flexible risers with irregular seas and hysteresis". In: Offshore Technology Conference (OTC), Houston, USA.

Torres, A. L. F. L.; Mourelle, M. M.; Senra S. F.; Gonzalez E. C.; Lima, J. M. T. G. (2008) - "Influence of fatigue issues on the design of SCRs for deepwater offshore Brazil". In: Offshore Technology Conference (OTC), Houston, USA, OTC-19249.

Vogel, M.; Silveira, I. C. A.; Castro, B. M.; Lima, J. A. M.; Pereira, A. F.; Williams, P. (2010) - "Metocean measurements at northern Santos basin - Brazil". In: Offshore Technology Conference (OTC), Houston, USA, OTC-20947.

Witz, A. J. (1996) - "A case study in the cross section analysis of flexible risers". Marine Structures, Volume 9, pages 885-904.

WAMIT (2012) - "A radiation-diffraction panel program for wave-body interaction". Report. Dept. of Ocean Eng., MIT, Cambridge, Mass., USA.

Wibner, C.; Versavel, T.; Masetti, I. (2003) - "Specifying and testing polyester mooring rope for the barracuda and Caratinga FPSO deep water mooring system". In: Offshore Technology Conference (OTC), Houston, USA, OTC-15139.